ISSN 0006-2979, Biochemistry (Moscow), 2009, Vol. 74, No. 2, pp. 175-185. © Pleiades Publishing, Ltd., 2009.
Original Russian Text © I. A. Vasil'eva, E. A. Semenova, N. A. Moor, 2009, published in Biokhimiya, 2009, Vol. 74, No. 2, pp. 216-228.
Originally published in Biochemistry (Moscow) On-Line Papers in Press, as Manuscript BM08-212, December 21, 2008.

Interaction of Human Phenylalanyl-tRNA Synthetase with Specific tRNA According to Thiophosphate Footprinting

I. A. Vasil'eva[1], E. A. Semenova[2], and N. A. Moor[1]*

[1]*Institute of Chemical Biology and Fundamental Medicine, Siberian Branch of the Russian Academy of Sciences, pr. Lavrentieva 8, 630090 Novosibirsk, Russia; fax: (383) 333-3677; E-mail: moor@niboch.nsc.ru*
[2]*Novosibirsk State University, ul. Pirogova 2, 630090 Novosibirsk, Russia*

Received June 23, 2008
Revision received July 10, 2008

Abstract—The interaction of human cytoplasmic phenylalanyl-tRNA synthetase (an enzyme with yet unknown 3D-structure) with homologous $tRNA^{Phe}$ under functional conditions was studied by footprinting based on iodine cleavage of thiophosphate-substituted tRNA transcripts. Most $tRNA^{Phe}$ nucleotides recognized by the enzyme in the anticodon (G34), anticodon stem (G30–C40, A31–U39), and D-loop (G20) have effectively or moderately protected phosphates. Other important specificity elements (A35 and A36) were found to form weak nonspecific contacts. The D-stem, T-arm, and acceptor stem are also among continuous contacts of the $tRNA^{Phe}$ backbone with the enzyme, thus suggesting the presence of additional recognition elements in these regions. The data indicate that mechanisms of interaction between phenylalanyl-tRNA synthetases and specific tRNAs are different in prokaryotes and eukaryotes.

DOI: 10.1134/S0006297909020084

Key words: nucleoside-5′-O-(1-thiotriphosphate), $tRNA^{Phe}$, human phenylalanyl-tRNA synthetase, footprinting

The structure of human cytoplasmic phenylalanyl-tRNA synthetase (PheRS) is one of the most complex in the family of aminoacyl-tRNA synthetases (aaRSs). The subunit structure of the cytoplasmic enzyme is evolutionally conservative and has molecular topology of $(\alpha\beta)_2$ type [1]. The main elements of $tRNA^{Phe}$ identity with various PheRSs of pro- and eukaryotic origin (including human) have been identified using mutant transcripts; the mechanism of $tRNA^{Phe}$ recognition by *T. thermophilus* enzyme at various stages of interaction has been studied in detail by X-ray structural analysis and functional methods [1, 2]. Nucleotides of the anticodon, the main elements of $tRNA^{Phe}$ specificity in all the studied systems, are recognized by the C-terminal domain of β-subunit (B8), which has a unique structural topology and is conservative in eubacterial enzymes. The absence of this domain in cytoplasmic PheRSs of eukaryotes and low homology of other tRNA-binding domains of α- and β-subunits [1] suggest that the mechanisms of enzyme interaction with $tRNA^{Phe}$ are different in pro- and eukaryotes. Functional and structural analysis of the enzymes most important for protein biosynthesis in higher eukaryotes, primarily human in comparison with the earlier studied bacterial systems, is especially important because aaRSs are considered as potential pharmaceutical targets [3, 4]. So far the 3D-structures of two human cytoplasmic aaRSs (mini-forms) specific to tyrosine (TyrRS) and tryptophan (TrpRS) [5, 6], human lysyl-tRNA synthetase (LysRS) (in a complex with protein p38) [7], and human mitochondrial TyrRS (in a complex with an analog of aminoacyladenylate, an intermediate product of the aminoacylation reaction) [8] have been determined, and structural data on the interaction with tRNA and small substrates have been obtained for human cytoplasmic TrpRS [9, 10].

To identify the contacts of human $tRNA^{Phe}$ with cytoplasmic PheRS, we used footprinting based on iodine cleavage of thiophosphate-substituted tRNAs. This method developed for chemical mapping of tRNA-synthetase complexes [11] appeared to be effective for study-

Abbreviations: aaRS, aminoacyl-tRNA synthetase; Phe-AMP, L-phenylalanyl-5′-adenylate; PheOH-AMP, L-phenylalaninyl-5′-adenylate; PheRS, phenylalanyl-tRNA synthetase (analogous abbreviations are used for other aminoacyl-tRNA synthetases with given specificity according to the commonly accepted amino acid notation).

* To whom correspondence should be addressed.

ing these and other systems [12-15]. Comparative analysis of our data with those for phenylalanine-specific systems from yeast [16] and *T. thermophilus* [17, 18] indicates that the mechanisms of PheRSs interaction with specific tRNAs are different in eubacteria and eukaryotes.

MATERIALS AND METHODS

The following reagents were used: ATP, UTP, GTP, and CTP from Fluka (Switzerland); uridilyl-(3′-5′)-guanosine (UpG) and dithiothreitol from Serva (Germany); ammonium persulfate from Merck (Germany); Tris, EDTA, and urea from ICN (USA); acrylamide from Helicon (Russia); N,N′-methylenebisacrylamide from Amresco (Greece); [γ-^{32}P]ATP and [5′-^{32}P]cytidine-3′,5′-diphosphate ([5′-^{32}P]pCp) (specific radioactivity ~140 TBq/mmol) produced in the Institute of Chemical Biology and Fundamental Medicine, Siberian Branch of the Russian Academy of Sciences (ICBFM SB RAS), L-[^{14}C]phenylalanine (13 GBq/mmol) from UVVVR (Czech Republic); L-[^{3}H]phenylalanine (2 TBq/mmol) from Amersham Biosciences (USA). α-Thiophosphate-substituted nucleoside triphosphate derivatives (ATPαS, UTPαS, GTPαS, and CTPαS) were synthesized by V. N. Sil'nikov (ICBFM SB RAS). L-Phenylalaninyl-5′-adenylate (PheOH-AMP) was synthesized as described earlier [19]. A plasmid with inserted human tRNA^{Phe} gene was constructed in the laboratory of Prof. O. Uhlenbeck (University of Colorado, USA). The total tRNA from *E. coli* MRE-600 was from Reakhim (Russia). T4 polynucleotide kinase was kindly given by I. O. Petruseva (ICBFM SB RAS); T4 RNA ligase was from Pharmacia Biotech (USA), and ribonuclease inhibitor was from Promega (USA). Human recombinant PheRS was isolated as described in [20]. LysRS *T. thermophilus* and recombinant T7 RNA polymerase were isolated by V. N. Ankilova (ICBFM SB RAS).

Transcripts corresponding to human tRNA^{Phe} sequence were synthesized *in vitro* using T7 RNA polymerase as described in [21]. To synthesize tRNA^{Phe} transcripts statistically substituted by thiophosphate residues at A-, G-, U-, or C-position, corresponding nucleoside triphosphate was added as a mixture of 0.05 mM nucleoside-5′-O-(1-thiotriphosphate) and 0.95 mM natural nucleotide. At such concentration ratio, the synthesized tRNAs on the average contain about one thiophosphate nucleotide per molecule, which is uniformly included during transcription [11, 17, 22].

Transcript of tRNA^{Phe} and its thiophosphate-substituted analogs were aminoacylated by human phenylalanyl-tRNA synthetase at 25°C as described earlier [20]. To determine K_m and V_{max} values, five different concentrations of tRNA substrate (from 0.1 to 1.2 μM) were used. Kinetic parameters were calculated using Microcal Origin 7.0 software; the standard errors did not exceed 10 and 5% for K_m and V_{max}, respectively.

^{32}P-Labeling of tRNA at the 5′-end was performed as described in [23] but with some modifications using tRNA^{Phe} transcript synthesized in the presence of 1 mM UpG. The ^{32}P-label was incorporated at the 3′-end of tRNA by addition of [5′-^{32}P]pCp to tRNA^{Phe} transcript using T4 RNA ligase as described in [24].

Iodine cleavage of thiophosphate-substituted tRNA^{Phe} analogs. The ^{32}P-labeled thiophosphate-substituted tRNA^{Phe}s were cleaved by iodine in the absence or in the presence of human PheRS as described in [11, 17] but with some modifications. The enzyme was pre-dialyzed against footprinting buffer (10 mM Tris-HCl, pH 8.1, containing 10 mM NaCl and 10 mM $MgCl_2$) using Microcon YM-10 ultrafiltration devices. The reaction mixture (10 μl) containing labeled (~30,000 cpm) and unlabeled thiophosphate tRNA^{Phe} at the total concentration 1 μM, 10 mM Tris-HCl (pH 8.1), 10-30 mM $MgCl_2$, 10-100 mM NaCl in the absence or in the presence of 1-7 μM human PheRS was incubated for 3 min at 25°C. In certain experiments, the reaction mixture additionally contained 0.1 mM PheOH-AMP and LysRS *T. thermophilus* (3 μM) instead of human PheRS. Then 1 μl of 1-10 mM I_2 dissolved in ethanol was added to the reaction mixture, which was incubated for 0.5-2 min; the reaction was stopped by addition of 0.4 M NaOAc buffer (pH 6.0) to 0.3 M concentration. The enzyme was removed by phenol extraction using an equal volume of phenol–chloroform mixture. After cleavage tRNA fragments were precipitated with 96% ethanol, the precipitate was separated by centrifugation and dried. The products of hydrolysis and tRNA were electrophoresed in 15% polyacrylamide gel under denaturing conditions using buffer with salt gradient as described in [25]; Bromphenol Blue was allowed to migrate in gel to 32 cm. To determine the length of RNA fragments, alkaline and nuclease (T1) tRNA hydrolyzates obtained as described in [23, 25] were used as markers. The gel was dried and visualized by autoradiography and scanning by Molecular Imager; Quantity One software was used for the data processing.

RESULTS AND DISCUSSION

Aminoacylation of thiophosphate-substituted human tRNA^{Phe} analogs. The substrate properties of thiophosphate-substituted tRNA^{Phe} derivatives synthesized under conditions for obtaining monosubstituted analogs were compared with corresponding properties of unsubstituted tRNA^{Phe} (Fig. 1 and table). (s-pG)tRNA^{Phe} and (s-pA)tRNA^{Phe} were aminoacylated with the same K_m and V_{max} values as unsubstituted tRNA^{Phe}. Specific acceptor activities and initial reaction rates of aminoacylation of four different thiophosphate-substituted tRNA^{Phe}s and unsubstituted transcript measured under identical condi-

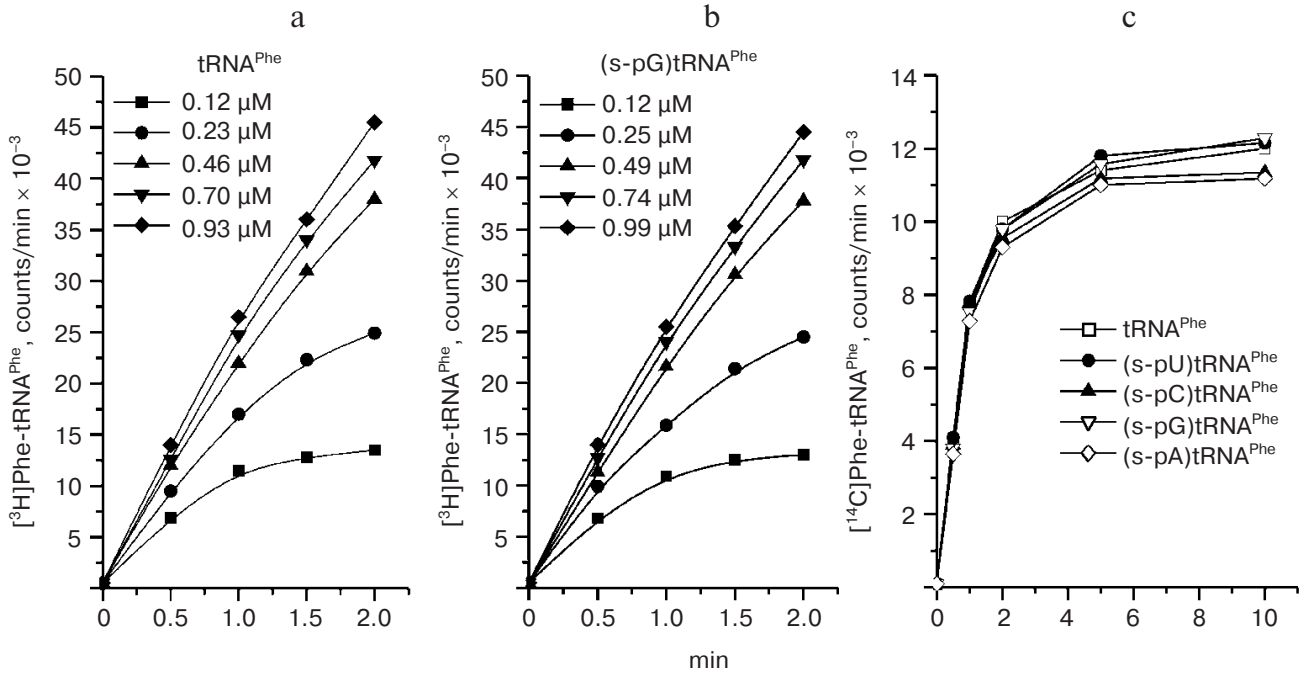

Fig. 1. Kinetic curves of aminoacylation of $tRNA^{Phe}$ transcript and its thiophosphate analogs by human phenylalanyl-tRNA synthetase. The reaction mixtures contained tRNA substrate at various concentrations (from 0.12 to 0.99 μM), 10 μM [^{3}H]Phe, 5 μg/ml enzyme (a, b) or 1.5 A_{260} unit/ml $tRNA^{Phe}$ transcript (thiophosphate-substituted or unsubstituted), 10 μM L-[^{14}C]Phe, 15 μg/ml enzyme (c), and other components as described in [20].

tions are comparable. Thus, $tRNA^{Phe}$ modification by statistical inclusion of nucleoside-5′-thiophosphate at positions corresponding to A, G, U, or C (under conditions for preferential synthesis of thiophosphate-monosubstituted transcript) does not influence its interaction with the enzyme.

Iodine cleavage of thiophosphate-substituted $tRNA^{Phe}$ analogs. The data on iodine cleavage of 5′-^{32}P-labeled thiophosphate-substituted $tRNA^{Phe}$s are presented in Fig. 2a. The tested phosphates are at the 5′-position of thiophosphate-substituted nucleotides. The sets of the main fragments of hydrolysis—(s-pA)-, (s-pU)-, (s-pG)-, or (s-pC)tRNA—correspond with positions of A-, U-, G-, and C-nucleotides in the $tRNA^{Phe}$ transcript sequence (Fig. 2b); this indicates specific cleavage at the thiophosphate groups. The total yield of cleavage at certain specific positions is 6-11%. The relative efficiency of cleavage at each position was calculated as the fraction of a fragment of corresponding length in the total radioactive sample. Significant differences in the cleavage efficiency

Kinetic parameters of aminoacylation of thiophosphate-substituted analogs of human $tRNA^{Phe}$ with homologous PheRS

$tRNA^{Phe}$ [a]	K_m^b, μM	V_{max}^b, nmol/min per mg	V_{max}/K_m^c, relative units	Maximum charging capacity of aminoacylation, pmol/A_{260} unit[d]
$tRNA^{Phe}$	0.16 ± 0.014	56 ± 2	1.0	1690 ± 20
(s-pU)$tRNA^{Phe}$				1770 ± 80
(s-pC)$tRNA^{Phe}$				1690 ± 70
(s-pG)$tRNA^{Phe}$	0.17 ± 0.010	56 ± 1	0.94	1720 ± 20
(s-pA)$tRNA^{Phe}$	0.16 ± 0.013	55 ± 1	0.98	1690 ± 40

[a] Human $tRNA^{Phe}$ and its thiophosphate-substituted analogs were synthesized by *in vitro* transcription.
[b] Parameters are given with standard errors.
[c] Values are normalized to corresponding value for thiophosphate-free $tRNA^{Phe}$.
[d] Average value for four measurements is given with standard deviation.

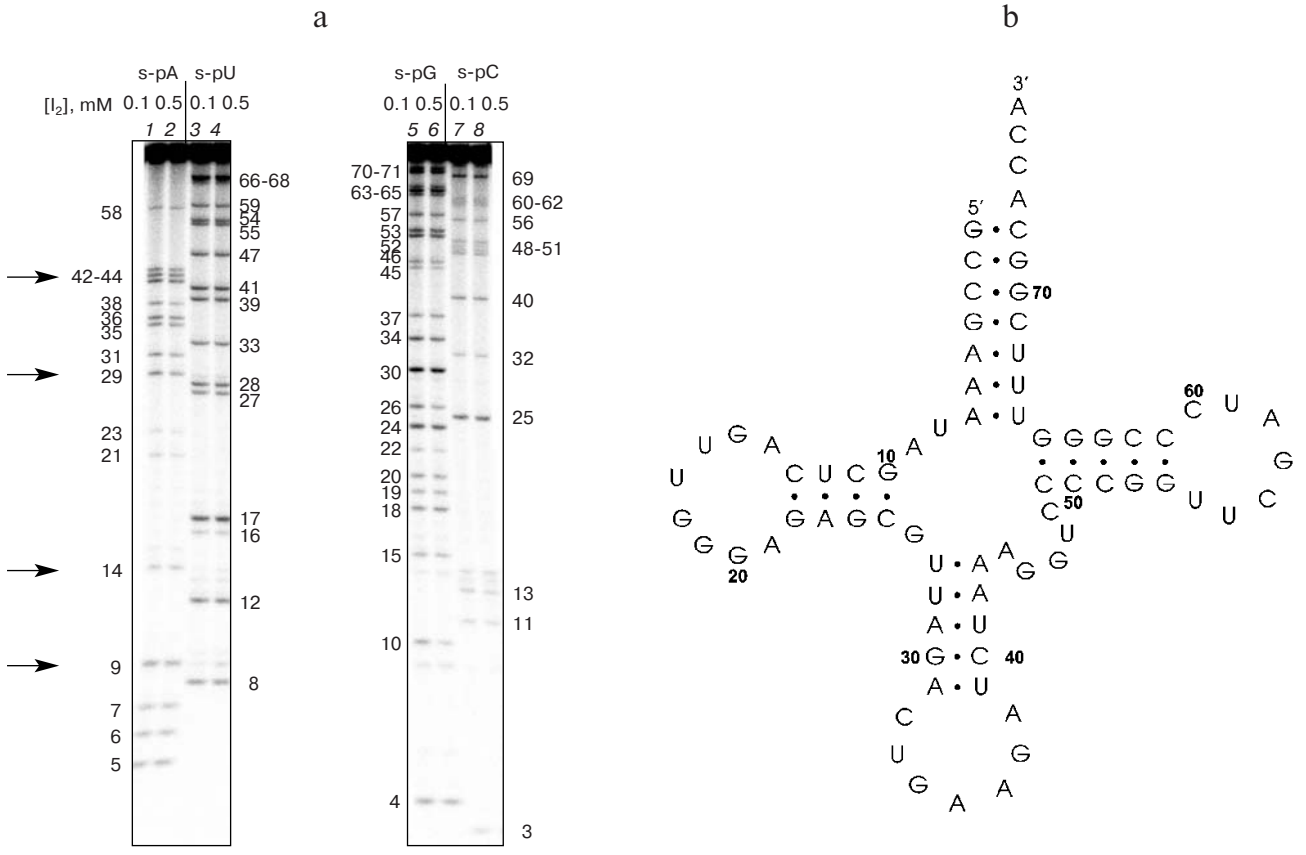

Fig. 2. a) Separation of the products of iodine cleavage of 5′-^{32}P-labeled thiophosphate-substituted analogs of human tRNA^{Phe} in polyacrylamide gel with urea. The reaction mixture contained 1 μM tRNA^{Phe} analog and 0.1 or 0.5 mM I_2; incubation time 2 min. Blocks designated as s-pA, s-pU, s-pG, and s-pC demonstrate the cleavage spectrum of tRNA^{Phe} containing the corresponding thiophosphate; nonspecific cleavage positions are marked by arrows. b) The secondary structure of human tRNA^{Phe} transcript.

for neighboring positions (in equally resolved regions) indicate that accessibilities of various sites of tRNA^{Phe} ribosophosphate backbone for the reagent are not equal. Cleavage efficiency at all positions was almost independent of the reaction time (from 2 to 10 min, data not presented here) and I_2 concentration (from 0.1 to 0.5 mM, Fig. 2a). Minor bands at positions 9, 14, 29, and 42 (Fig. 2a, marked by arrows) were observed in all experiments including the control with unsubstituted transcript in the presence as well as in the absence of I_2 (data not presented here); these bands correspond to nonspecific tRNA cleavage. The earlier described formation of similar products is caused by the initial bond instability in the structures of tRNA transcripts [11, 26, 27]. The observed nonspecific cleavage sites are located in CpA and UpA sequences most susceptible to the spontaneous cleavage [28].

Identification of contact sites of tRNA^{Phe} with human PheRS. To identify contact sites of human tRNA^{Phe} in a complex with homologous PheRS, we compared the cleavage efficiency at each tRNA^{Phe} position in the presence and in the absence of the enzyme. The hydrolysis reaction conditions used for footprinting were optimized in preliminary experiments at the varied concentrations of components (data not presented here) so that to provide the most effective tRNA binding to the enzyme and to reveal all contacts including weak interactions. At low I_2 concentrations (0.1 mM) additional protected positions appeared; at I_2 concentrations 0.5-1 mM the enzyme was inactivated. Analogous data in [11] indicate that protective effect of the enzyme depends on concentration of cleaving reagent. Varied concentrations of NaCl (10-100 mM) and $MgCl_2$ (10-30 mM) on which stability of tRNA-synthetase complexes and the tertiary structure of tRNA transcripts [29-31] depend negligibly influenced the observed phenomena. At the fixed tRNA^{Phe} concentration (1 μM), increased protective effect of the enzyme was observed on concentration increase from 1 to 3 μM; this correlates with increased extent of tRNA binding (the dissociation constant of the studied complex K_d ~ 2 μM) [21, 32]. The following concentrations of components were chosen as optimal ones: 0.1 mM I_2, 10 mM NaCl, 10 mM $MgCl_2$, 1 μM tRNA^{Phe} transcript, and 3 μM PheRS.

The data on separation of the fragments of hydrolysis of 5′-^{32}P-labeled thiophosphate derivatives in the absence and in the presence of PheRS are presented in Fig. 3. When 5′-labeled tRNAs are used, nucleotides at position 4-64 are in a well-resolved area. To reliably identify the enzyme contacts with the 3′-terminal region (65-71), we performed additional experiments with the 3′-labeled tRNAs. The observed effects (a) and schematic presentation of results on the secondary (b) and tertiary (c) structures of human tRNA^{Phe} are depicted in Fig. 4. For the protected phosphate residues in contact with the enzyme, cleavage efficiency decreases. An opposite effect—increased cleavage efficiency in the presence of PheRS—indicates that formation of a complex induces conformational changes in the tRNA. Changes in hydrolysis efficiency exceeding 25% (accounting for experimental errors given in the histogram) were considered as meaningful. The most pronounced cleavage suppression (2-3 times) in the presence of PheRS was observed for phosphates at positions 24, 25, 26 of the D-arm, and 30 and 41 of the anticodon arm. The average level of protection by the enzyme (1.5-1.9-times decrease in cleavage efficiency) was found for phosphates at positions 5, 66, 68, and 69 of the acceptor stem; 20 of the D-arm; 27, 28, 29, 31, 34, 38, and 42 of the anticodon arm; 52, 53, 54, 55, and 64 of the T-arm. Weak suppression of cleavage (from 1.3 to 1.5-times) was observed for phosphates at positions 6 and 67 of the acceptor stem; 12 and 23 of the D-arm; 33, 35, 36, and 43 of the anticodon arm; 44 and 47 of the V-loop; 57, 59, 63, and 65 of the T-arm.

Thus, the most stable continuous contacts of human PheRS with tRNA^{Phe} ribosophosphate backbone are localized at the 3′-side of the D-stem, both sides of the anticodon arm, the 5′-side of T-stem, and in the junction region of the T- and acceptor arms. Noticeable increase in the cleavage efficiency (1.3-1.7 times) is observed at positions 9, 14, 16, and 17, which possibly indicates conformational changes in corresponding tRNA regions in a complex with the enzyme; these changes increase accessibility of the attacked thiophosphate groups for the reagent. Nonspecific spontaneous cleavage of tRNA observed in the absence of PheRS at positions 9, 14, 29, and 42 (marked by black arrows in Figs. 3 and 4) is retained also in the presence of the enzyme. The observed effect of human PheRS on cleavage of thiophosphate-containing tRNA^{Phe} indicates interactions in the specific complex; in analogous experiments with *T. thermophilus* LysRS neither protective effect nor enhanced cleavage was found at any of the positions.

The influence of the enzyme on cleavage of thiophosphate-substituted human tRNA^{Phe} was studied in the absence or in the presence of stable aminoacyladenylate analog PheOH-AMP containing the methylene group instead of carbonyl (Fig. 3). For positions 24, 25, and 30, the protective effect decreased 1.3-1.5-fold in the presence of PheOH-AMP. In contrast, the protective

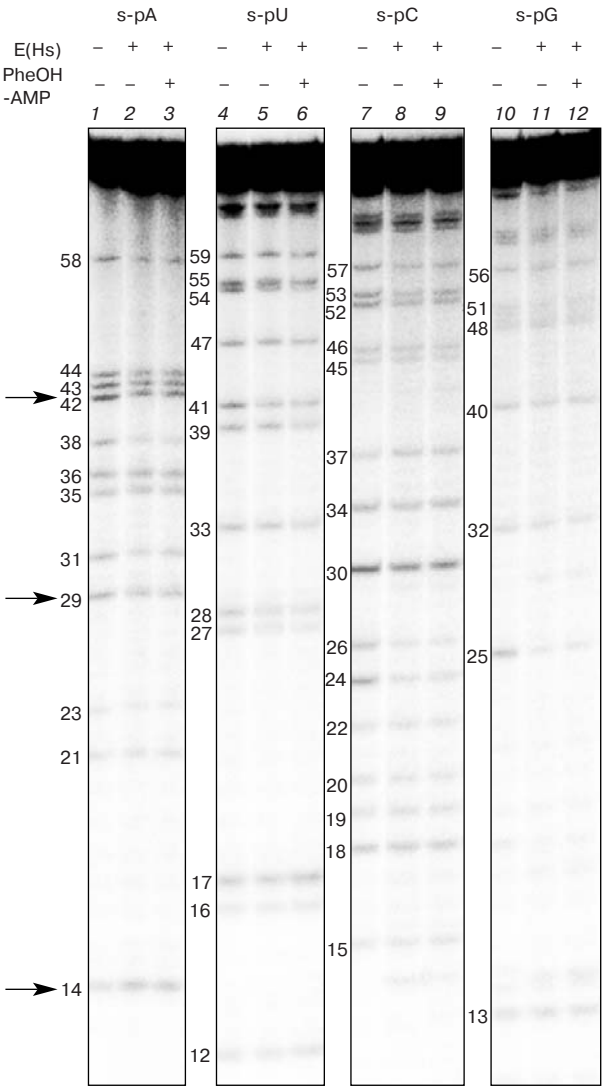

Fig. 3. Iodine cleavage of 5′-^{32}P-labeled thiophosphate-substituted analogs of human tRNA^{Phe} in the absence (lanes *1*, *4*, *7*, *10*) or in the presence (lanes *2*, *3*, *5*, *6*, *8*, *9*, *11*, *12*) of human PheRS (E(Hs)) and in the presence of PheOH-AMP (lanes *3*, *6*, *9*, *12*). The reaction mixture contained 1 μM thiophosphate-substituted tRNA^{Phe}, 0.1 mM I_2, 3 μM enzyme, 0.1 mM PheOH-AMP; reaction time 2 min. Positions of nonspecific cleavage are marked by arrows.

effect of the enzyme at position 10 increased 1.5-fold in the triple complex PheRS·tRNA^{Phe}·PheOH-AMP. All the nucleotides at the mentioned positions are concentrated in one region of the continuous double helix formed by the anticodon and D-arms. In general, the effect of aminoacyladenylate analog is not significant but selective in relation to certain regions. To prove its functional significance and participation of the D-arm and anticodon arm in the structural rearrangements of human PheRS·tRNA^{Phe} complex induced by PheOH-AMP binding to the active site, additional studies by independent methods are required.

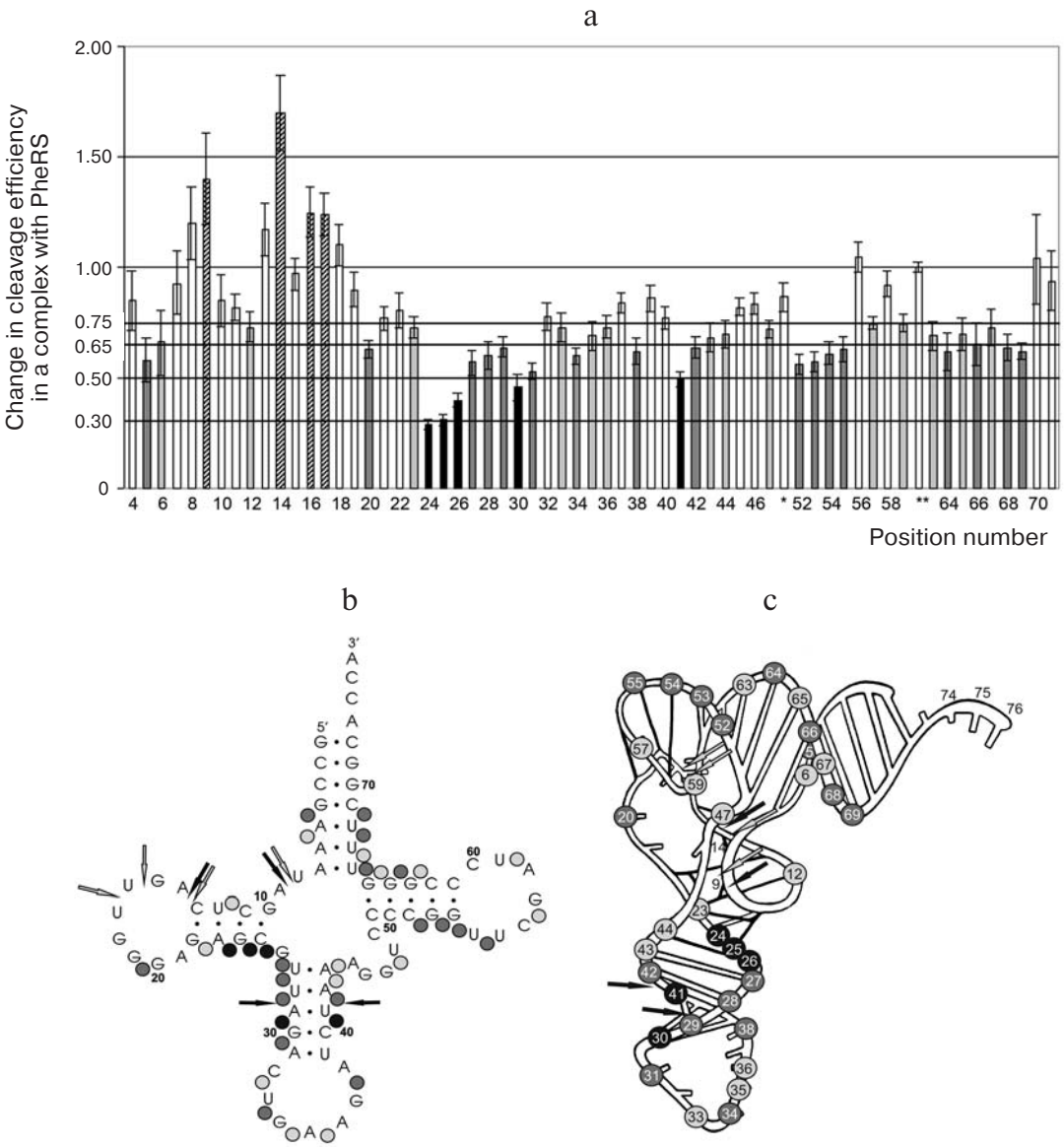

Fig. 4. Effect of human PheRS on hydrolysis of $tRNA^{Phe}$ thiophosphate derivatives. a) Histogram showing a ratio of hydrolysis efficiency at each position in the complex to the corresponding value in the absence of enzyme; the average values of eight independent experiments (with 5′- and 3′-labeled tRNA transcripts) and their standard deviations (6-14% for positions 7-69 and 15-23% for extreme positions) are given. b, c) Schematic presentation of the footprinting data on the secondary or tertiary $tRNA^{Phe}$ structure. Positions for which significant (~2 times and more), average (1.5-1.9 times), and weak (less than 1.5 times) protective effects were observed are shown by black, gray, and light-gray columns (a) and circles (b, c), respectively; positions of enhanced cleavage in the complex are shown by black diagonal dashing of columns (a) and gray arrows (b, c); sites of spontaneous cleavage are marked by black arrows (b, c). Badly resolved positions (analyzed as one band) are marked by asterisks.

Comparison of footprinting data with data on recognition elements. Three nucleotides of the anticodon, discriminatory base A73 in the acceptor arm, G20 in the D-loop, and two pairs of the anticodon stem (G30–C40, A31–U39) are the main elements of specificity in the studied system [33]. A noticeable contribution of the anticodon stem to tRNA recognition is a characteristic feature of human Phe-specific system [1]. One nucleotide of the anticodon (G34), both pairs of the anticodon stem (G30–C40, A31–U39), and G20 in the D-stem are the recognition elements in the regions of close nonspecific contacts detected by thiophosphate footprinting and protected to a high or medium extent. Weak protection of the phosphate groups A35 and A36 indicates that significant contribution of these nucleotides to $tRNA^{Phe}$ recognition by the enzyme is most probably caused by participation of bases in a complex formation. However, extended contacts with enzyme are localized in the D- and acceptor

stems, and also in the T-arm; this does not exclude the presence of additional recognition elements in these regions that were not detected earlier using a limited number of mutant $tRNA^{Phe}$s. Besides the anticodon arm, only the D-arm and two positions of the T-loop (59 and 60) are the studied regions [33]. Single replacements of tertiary nucleotides (G26, A44 and C25, G10, and G45) forming the G26–A44 tertiary pair and C25–G10–G45 triple resulted in two-fold decrease in catalytic efficiency of aminoacylation [33]. Four of these participate in contacts of the sugar-phosphate backbone with the enzyme and can make a minor contribution to recognition of general architecture of $tRNA^{Phe}$, as shown for Phe-specific pairs of *E. coli* and *T. thermophilus* [1, 2]. A73 is located in the unresolved area, and detection of possible contacts in these regions requires additional studies by other methods.

Interaction of phenylalanyl-tRNA synthetases of various origins with homologous $tRNA^{Phe}$s. To compare our data with the data on other $tRNA^{Phe}$–PheRS pairs, the latter are presented in Fig. 5. Structure of a complex of yeast $tRNA^{Phe}$ with homologous PheRS was analyzed using an alkylation reagent (ethylnitrosourea) [16], and the structure of the complex of *T. thermophilus* $tRNA^{Phe}$ with homologous PheRS was analyzed using iodine-induced hydrolysis [17]. For two eukaryotic systems studied using various reagents, the regions protected from cleavage by the enzyme are more similar than for bacterial and eukaryotic systems studied by the same (thiophosphate) method (for comparison, see Fig. 4).

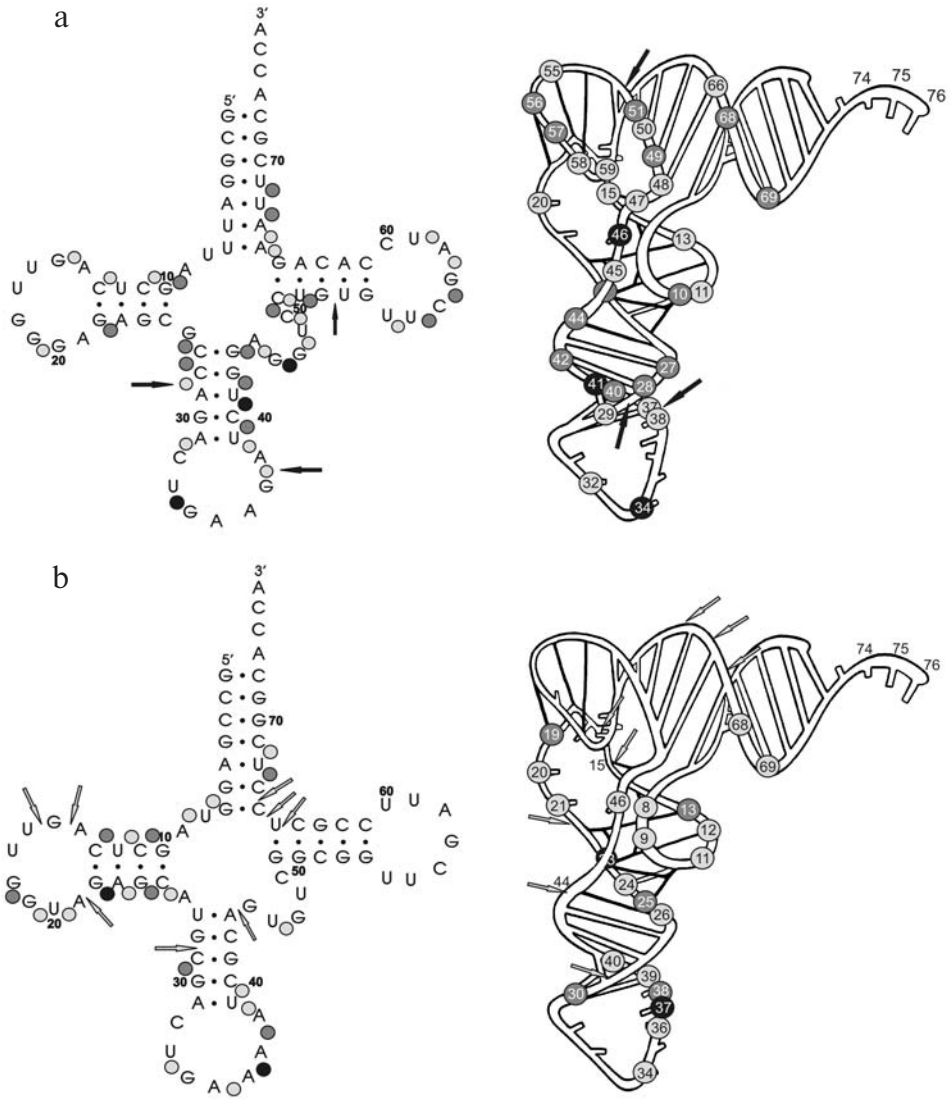

Fig. 5. Regions of nonspecific contacts of $tRNA^{Phe}$ of yeast (a) and *T. thermophilus* (b) with corresponding PheRSs identified by chemical footprinting [16, 17]. In the secondary and tertiary $tRNA^{Phe}$ structures, positions, for which high, medium, and weak protective effects are detected, are shown by black, gray, and light-gray circles, respectively. Positions, at which cleavage in a complex is enhanced, are marked by gray arrows, and the sites of spontaneous cleavage are marked by black arrows.

The extended continuous nonspecific contacts of $tRNA^{Phe}$ involving two sides of the anticodon arm, the base-paired region of T-arm, and more extended contacts with the acceptor stem are typical of eukaryotic tRNA–synthetase pairs. For eukaryotic systems, some difference at a particular contact position and in the degree of effect might be caused by different types of reagents and experimental conditions, more stable structure of natural yeast $tRNA^{Phe}$ compared with that of human $tRNA^{Phe}$ transcript (used in corresponding experiments), and also insufficient resolution of the acceptor arm regions [16].

Continuous contacts between $tRNA^{Phe}$ and PheRS of *T. thermophilus* were identified by footprinting only for the 3′-side of the anticodon arm; no contacts at all were detected for the T-arm. All of the anticodon arm, the 5′-side of the T-stem, and the junction region of the T-arm and acceptor arm participate in formation of extended contacts between $tRNA^{Phe}$ and human PheRS. The interaction with the D-arm and acceptor stem are also different: in the eukaryotic system the most pronounced protective effects are detected only for the 3′-side of the D-arm and for the phosphate residues in the bottom of the acceptor stem, whereas in the bacterial system pronounced protective effects are detected for all the D-arm and for only two phosphate residues of the 3′-side of the acceptor arm. It should be noted that the effect of *T. thermophilus* PheRS on tRNA cleavage is more significant than that of human PheRS. A 5-10-, 2-5-, or 1.3-2-fold decreases in hydrolysis efficiency in the bacterial system were considered as high, medium, and weak protective effects, respectively [17]. Such difference in the two systems is caused, first of all, by stronger $tRNA^{Phe}$ binding to the bacterial enzyme: the dissociation constant of *T. thermophilus* PheRS complex with specific tRNA K_d = 5 nM is significantly lower than corresponding value (~2 μM) for the human Phe-specific pair [21, 23]. Formation of the most intensive nonspecific contacts between *T. thermophilus* $tRNA^{Phe}$ and homologous enzyme with participation of the D-arm is shown also by X-ray structural analysis of the complex [18]. In the crystal structure the upper part of the anticodon stem and C56 of the T-loop participate in nonspecific contacts not detected by footprinting. This difference in biochemical and structural data indicates that not all contacts between protein and ribosophosphate backbone can be revealed by the method used. The latter allows to detect close protein contacts with the phosphate groups at the side of sulfur atoms, which are turned inside the major groove of the double helix in accord with the R_p-configuration of the thiophosphate groups [17].

Comparative analysis of amino acid sequences of PheRS from various organisms [32] demonstrated significant difference between enzymes of different origin (Fig. 6). Two domains of the large β-subunit—the C-terminal domain B8 and domain B2 forming an insertion into the N-terminal domain B1—are highly conservative in eubacterial PheRSs. These domains are absent from analogous cytoplasmic enzymes in eukaryotes. The catalytic α-subunit of eukaryotic PheRSs is markedly elongated at the N-terminus; this possibly indicates significant (almost 2-fold) increase in dimension of the N-terminal domain forming a coiled-coil domain (CC) in *T. thermophilus* PheRS. Interactions of B8 and CC domains with various regions of $tRNA^{Phe}$ mainly contribute to the substrate recognition [1, 34]. Other domains participating in $tRNA^{Phe}$ binding—B1, B3, B6, and B7—are conservative in PheRSs of various origins, along with the catalytic module A1-A2 and domain B5. Domains B1, B3, B5, B6, and B7 participate in α/β-intersubunit interactions stabilizing the active site structure [1]. The conservative nature of most domains suggests that pro- and eukaryotic PheRSs are similar in general organization of the 3D structure. Based on this suggestion, we analyzed what domains might potentially participate in formation of contacts revealed for human $tRNA^{Phe}$.

The structure of *T. thermophilus* PheRS complex with $tRNA^{Phe}$ is presented in Fig. 7. The anticodon arm of $tRNA^{Phe}$ in the complex with the bacterial enzyme is localized ("clamped") between two domains: domain B8 interacts with the double helix formed by the anticodon and D-arms, at the internal side of L-form, and domain CC at the opposite side. All nucleotides of the T-arm, for which the contacts typical only for eukaryotic system are revealed, are localized at the CC-domain side in the complex structure. Thus, this domain significantly elongated in human PheRS (Fig. 6) most probably participates in binding not only to the anticodon stem, variable loop, and G19–C56 pair at the corner of the L-form (as in the bacterial system), but to all the T-arm. The B6–B7 module can participate in interactions with nucleotides of the D-stem as well as in the complex with bacterial PheRS. Function of the absent B8 domain responsible for binding to the anticodon loop and D-stem is most probably fulfilled by the elongated N-terminus of the CC domain. It should be noted that this domain of PheRS has the most flexible conformation: its orientation in the 3D-structure of protein is stabilized by interactions with tRNA [18, 34]. The junction region of the acceptor and T-arms and nucleotides at positions 5, 6, 64, and 65 are localized at a large distance from all domains (Fig. 7): for their binding, a significant change in mutual orientation of tRNA and protein domains is required. In fact, the structural data on the fragment of β-subunit of archeabacterial PheRS (structurally homologous to eukaryotic enzymes) indicate that this enzyme differs from *T. thermophilus* PheRS in orientation of B3 and B4 domains in relation to the B1 and B5 domains [35]. The evolutionarily conservative way of binding of the acceptor end of $tRNA^{Phe}$ by *T. thermophilus* and human PheRSs in the contact area of α- and β-subunits is demonstrated by affinity modification: the 3′-terminal

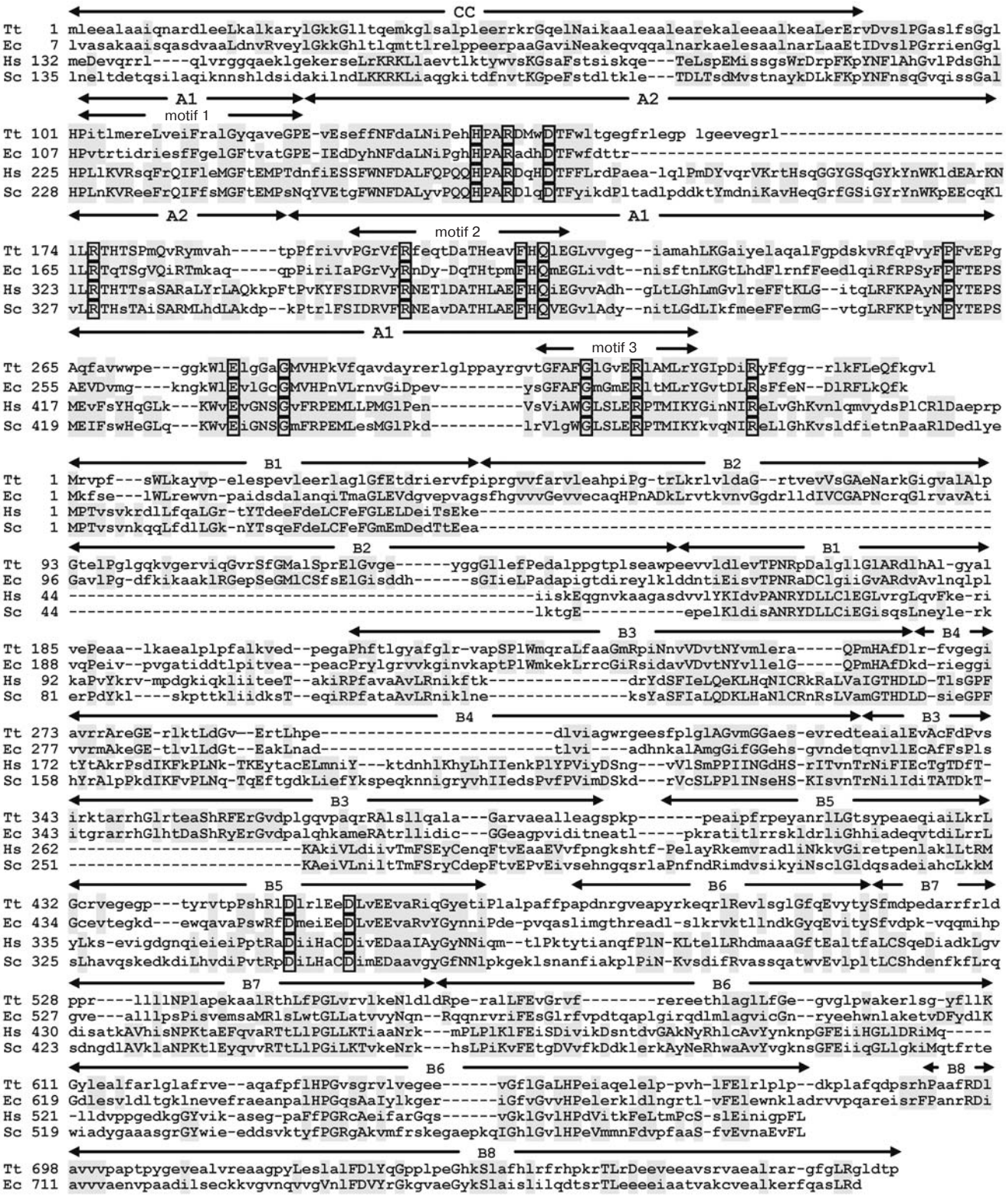

Fig. 6. Comparison of sequences of tetrameric PheRSs from various organisms: *Thermus thermophilus* (Tt), *Escherichia coli* (Ec), *Homo sapiens* (Hs), *Saccharomyces cerevisiae* (Sc). Composition of domains and signature motifs of the class II synthetases are shown above the sequences. Amino acid residues conservative (identical or structurally similar) in eubacterial or eukaryotic PheRSs are marked on the gray background; universal residues are in the frames. A figure with modification is presented according to [32].

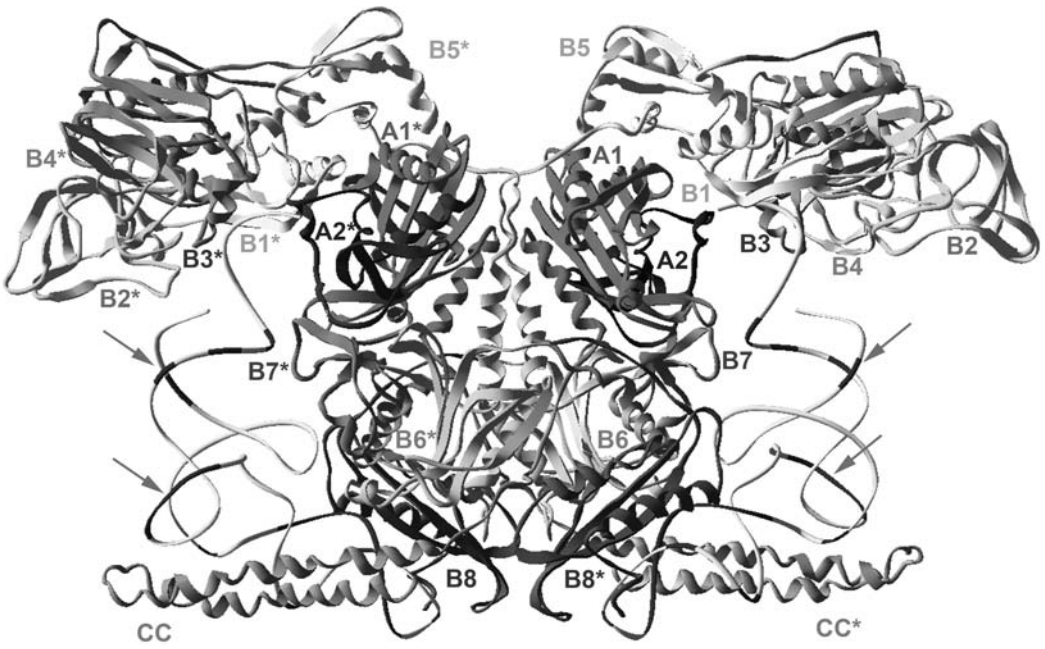

Fig. 7. General view of the 3D structure of *T. thermophilus* PheRS complex with homologous $tRNA^{Phe}$. Domains A1 and A2 forming the catalytic module and CC domain belong to α-subunit, whereas B1-B8 domains belong to β-subunit; domains of the second symmetry-related αβ-heterodimer are marked by an asterisk. According to the data on the thiophosphate footprinting of the corresponding complex, the nucleotide residues with phosphate groups protected by the human enzyme to high and medium extents are highlighted by dark gray on the tRNA structure (ribbon representation). Nucleotides localized at a large distance from all domains are shown by arrows. The images were generated using Swiss-PDB Viewer 3.7 software, PDB code 1EIY.

accepting nucleotide is localized on α-subunit, whereas the neighboring nucleotide of CCA-end – on β-subunit [32]. However, the kinetic data on aminoacylation of the mutant tRNAs indicate that the two enzymes interact in a different way with the acceptor arm of tRNA substrate: A73 negligibly contributes to recognition of bacterial $tRNA^{Phe}$ but is a major determinant of human $tRNA^{Phe}$ specificity [1].

The data suggest the evolutionarily conservative role of B6–B7 module of β-subunit and the N-terminal CC domain of α-subunit of eubacterial and eukaryotic PheRSs in formation of contacts with the central regions of $tRNA^{Phe}$, which provide substrate binding and recognition of its general architecture. The N-terminal domain of the α-subunit markedly elongated in eukaryotic PheRS also functions as the anticodon-recognizing domain. In general, the data indicate that specific complex of PheRS with tRNA substrate is formed in different ways in prokaryotes and eukaryotes.

The authors are grateful to Prof. M. Safro (Weizmann Institute, Israel) for kindly provided plasmids for expression of recombinant human PheRS and to Prof. O. I. Lavrik for a valuable discussion of the manuscript.

This work was financially supported by the Russian Foundation for Basic Research (grant No. 06-04-48798).

REFERENCES

1. Safro, M., Moor, N., and Lavrik, O. (2005) in *The Aminoacyl-tRNA Synthetases* (Ibba, M., Francklyn, C., and Cusack, S., eds.) Landes Bioscience, Georgetown, TX, pp. 250-265.
2. Vasil'eva, I. A., and Moor, N. A. (2007) *Biochemistry* (Moscow), **72**, 247-263.
3. Raczniak, G., Ibba, M., and Söll, D. (2001) *Toxicology*, **160**, 181-189.
4. Kron, M., and Härtlein, M. (2005) in *The Aminoacyl-tRNA Synthetases* (Ibba, M., Francklyn, C., and Cusack, S., eds.) Landes Bioscience, Georgetown, TX, pp. 397-404.
5. Yang, X.-L., Skene, R. J., Mcree, D. E., and Schimmel, P. (2002) *Proc. Natl. Acad. Sci. USA*, **99**, 15369-15374.
6. Yang, X.-L., Otero, F. J., Skene, R. J., Mcree, D. E., Schimmel, P., and de Pouplana, L. R. (2003) *Proc. Natl. Acad. Sci. USA*, **100**, 15376-15380.
7. Guo, M., Ignatov, M., Musier-Forsyth, K., Schimmel, P., and Yang, X. L. (2008) *Proc. Natl. Acad. Sci. USA*, **105**, 2331-2336.
8. Bonnefond, L., Frugier, M., Touzé, E., Lorber, B., Florentz, C., Giegé, R., Sauter, C., and Rudinger-Thirion, J. (2007) *Structure*, **15**, 1505-1516.
9. Yang, X.-L., Otero, F. J., Ewalt, K. L., Liu, J., Swairjo, M. A., Kohrer, C., RajBhandary, U. L., Skene, R. J., Mcree, D. E., and Schimmel, P. (2006) *EMBO J.*, **25**, 2919-2929.
10. Shen, N., Zhou, M., Yang, B., Yu, Y., Dong, X., and Ding, J. (2008) *Nucleic Acids Res.*, **36**, 1288-1299.

11. Schatz, D., Leberman, R., and Eckstein, F. (1991) *Proc. Natl. Acad. Sci. USA*, **88**, 61302-61306.
12. Giegé, R., and Frugier, M. (2003) in *Translation Mechanisms* (Lapointe, J., and Brakier-Gingras, L., eds.) Landes Bioscience, Georgetown, TX, pp. 1-24.
13. Dambowski, M., Junemann, R., Schafer, M. A., Spahn, C. M. T., Nierhaus, K. H., Alexeeva, E. V., Dontsova, O. A., Shpanchenko, O. V., and Bogdanov, A. A. (1996) *Biochemistry* (Moscow), **61**, 1402-1412.
14. Ming, X., Smith, K., Suga, H., and Hou, Y.-M. (2002) *J. Mol. Biol.*, **318**, 1207-1220.
15. Herring, S., Ambrogelly, A., Polycarpo, C. R., and Söll, D. (2007) *Nucleic Acids Res.*, **35**, 1270-1278.
16. Vlassov, V. V., Kern, D., Romby, P., Giegé, R., and Ebel, J.-P. (1983) *Eur. J. Biochem.*, **132**, 537-544.
17. Kreutzer, R., Kern, D., Giegé, R., and Rudinger, J. (1995) *Nucleic Acids Res.*, **23**, 4598-4602.
18. Goldgur, Y., Mosyak, L., Reshetnikova, L., Ankilova, V., Khodyreva, S., Lavrik, O., and Safro, M. (1997) *Structure*, **5**, 59-68.
19. Lavrik, O., Moor, N., and Nevinskii, G. (1978) *Bioorg. Khim.*, **4**, 1470-1487.
20. Moor, N., Linshiz, G., and Safro, M. (2002) *Protein Expr. Purif.*, **24**, 260-267.
21. Vasil'eva, I. A., Ankilova, V. N., Lavrik, O. I., and Moor, N. A. (2002) *J. Mol. Recognit.*, **15**, 188-196.
22. Ruffner, D. E., and Uhlenbeck, O. C. (1990) *Nucleic Acids Res.*, **18**, 6025-6029.
23. Silberklang, M., Gillum, A. M., and RajBhandary, U. L. (1979) *Meth. Enzymol.*, **59**, 58-109.
24. England, T. E., and Bruce, A. G. (1980) *Meth. Enzymol.*, **65**, 65-74.
25. Moor, N. A., Ankilova, V. N., Lavrik, O. I., and Favre, A. (2001) *Biochim. Biophys. Acta*, **1518**, 226-236.
26. Dock-Bregeon, A. C., Garcia, A., Giegé, R., and Moras, D. (1990) *Eur. J. Biochem.*, **188**, 283-290.
27. Horowitz, J., Chu, W. C., Derrick, W. B., Liu, J. C., Liu, M., and Yue, D. (1999) *Biochemistry*, **38**, 7737-7746.
28. Beresten, S., Jahn, M., and Söll, D. (1992) *Nucleic Acids Res.*, **20**, 1523-1530.
29. Krauss, G., Riesner, D., and Maass, G. (1976) *Eur. J. Biochem.*, **68**, 81-93.
30. Bonnet, J., and Ebel, J. P. (1975) *Eur. J. Biochem.*, **58**, 193-201.
31. Maglott, E. J., Sanmitra, S. D., Przykorska, A., and Glick, G. D. (1998) *Biochemistry*, **37**, 16349-16359.
32. Moor, N., Lavrik, O., Favre, A., and Safro, M. (2003) *Biochemistry*, **42**, 10697-10708.
33. Nazarenko, I. A., Tinkle-Peterson, E., Zakharova, O. D., Lavrik, O. I., and Uhlenbeck, O. C. (1992) *Nucleic Acids Res.*, **20**, 475-478.
34. Moor, N., Kotik-Kogan, O., Tworowski, D., Sukhanova, M., and Safro, M. (2006) *Biochemistry*, **45**, 10572-10583.
35. Sasaki, H. M., Sekine, S., Sengoku, T., Fukunaga, R., Hattori, M., Utsunomiya, Y., Kuroishi, C., Kuramitsu, S., Shirouzu, M., and Yokoyama, S. (2006) *Proc. Natl. Acad. Sci. USA*, **103**, 14744-14749.